# Reflectance of polyaniline protonated with camphor sulfonic acid: Disordered metal on the metal-insulator boundary

Kwanghee Lee and A. J. Heeger
*Institute for Polymers and Organic Solids and Department of Physics, University of California at Santa Barbara, Santa Barbara, California 93106*

Y. Cao
*UNIAX Corporation, 5375 Overpass Road, Santa Barbara, California 93111*
(Received 10 June 1993; revised manuscript received 23 August 1993)

Recent progress in the processing of conducting polyaniline (PANI) protonated with functionalized sulfonic acids [such as camphor sulfonic acid (CSA)] has enabled the fabrication of high-quality, homogeneous films with excellent surface quality. We present measurements of the reflectivity of such PANI-CSA films over a wide spectral range (0.006–6 eV) at temperatures from 10 to 300 K. The reflectance spectra of PANI-CSA are characterized by metal-like signatures in the infrared (IR), including high reflectance in far IR and a plasma resonance around 1.2 eV. However, the optical conductivity $\sigma(\omega)$ and the real part of the dielectric function, $\varepsilon_1(\omega)$, are not typical of a Drude metal; $\sigma(\omega)$ is suppressed below the Drude extrapolation as $\omega \rightarrow 0$ with a peak around 0.2 eV, and $\varepsilon_1(\omega) > 0$ below 0.2 eV. These features arise from disorder-induced localization (Anderson localization) in PANI-CSA. We present a quantitative analysis of $\sigma(\omega)$ and $\varepsilon_1(\omega)$ in terms of the localization-modified Drude model. The analysis indicates that the mean free path is approximately 7 Å, comparable to the structural repeat unit along the PANI chain, implying that PANI-CSA is a disordered metal on the metal-insulator boundary.

## I. INTRODUCTION

Within the class of conducting polymers,[1,2] polyaniline (PANI) is unique in that its electronic structure and electrical properties can be reversibly controlled both by charge-transfer doping and by protonation.[3] Moreover, PANI can be processed in both insulating (emeraldine base) and conducting (emeraldine salt) forms.[4,5] The wide range of associated electrical and optical properties, coupled with excellent environmental and thermal stability, make polyaniline attractive as an electronic material for potential use in a variety of applications.[4,5] Thus PANI has emerged as one of the most promising conducting polymers.

The protonation of the emeraldine base to the conducting emeraldine salt form leads to an electronic structure with one unpaired spin per formula unit, $(\text{-}\phi\text{-NH-}\phi\text{-NH-})^{+\bullet}$, where $\phi$ denotes a phenyl ring, N and H are nitrogen and hydrogen atoms, respectively, and the dot denotes an unpaired electron delocalized on the repeat unit.[4–6] Thus the electronic structure corresponds to that of a metal with the highest occupied band three quarters filled.[7] The observation of a temperature-independent Pauli susceptibility[8,9] and broad absorption extending throughout the infrared[10] indicate the existence of a degenerate electronic structure with a finite density of states at the Fermi energy, and with low-energy intraband excitations. The magnitude of the Pauli spin susceptibility[8,9] implies a density of states at the Fermi energy of approximately one state per eV per formula unit (two rings).

Although the protonated emeraldine salt is known to exhibit many properties characteristic of the metallic state, polyaniline typically does not exhibit the traditional signatures of metallic transport; a positive temperature coefficient of the resistivity ($d\rho/dT > 0$) and a thermoelectric power which is proportional to temperature ($S \propto T$). Instead, the conductivity was found to be activated, decreasing by several orders of magnitude as the temperature is lowered; and the thermopower showed a complex (nonmonotonic) temperature dependence.[4–6,11–18]

The "nonmetallic" temperature dependence of the resistivity and of the thermopower arise from a combination of *mesoscale inhomogeneity* associated with phase segregation[13] and/or with *molecular scale disorder*.[4,5] Both are introduced during the doping process, and are indicative of the quality of the material. As a result, the conducting form of PANI has been categorized either as a granular metal[19,20] containing "metallic islands,[13]" or a disordered conductor[5] in which the electronic states at the Fermi energy ($E_F$) are localized.

It is well known that disorder can induce the localization of states;[21–25] indeed, if the magnitude of the disorder potential is large compared with the bandwidth, all states become localized. Such a system will be an insulator, since the Fermi level lies in an energy interval in which all states are localized. If the disorder is not large enough to cause localization throughout the band, the localized and extended states are separated by the mobility edge ($E_C$). In such a system, the metal-insulator transition is defined by the position of $E_F$ relative to $E_C$; if $E_F$ lies in the region of extended states, the system will be a metal, whereas if $E_F$ lies in the region of localized states, the system will be a Fermi glass insulator. In the latter case, electronic transport takes place by variable range

 

hopping (VRH) (Ref. 25) between exponentially localized states with energies near $E_F$.

Functionalized sulfonic acids have recently been used to protonate PANI, and to induce solubility in the conducting form.[26,27] Solution processing of corresponding emeraldine salts (with surfactants as counterions) has greatly improved the homogeneity of the material and has resulted in a significant decrease in the extent of molecular scale disorder.[28,29]

The ability to process the conducting form of polyaniline from solution has enabled us to obtain high-quality free-standing films of PANI protonated with camphor sulfonic acid (CSA) appropriate for optical reflectance studies. We present the results of reflectivity measurements over a wide range of energies (0.006–6 eV) and temperatures (10–300 K); the optical constants were obtained via Kramers-Kronig analysis of the reflectivity spectra. The reflectance spectra of PANI-CSA are characterized by metal-like behavior. In the far IR, the reflectance is high, indicative of low-energy intraband excitations. A minimum in the reflectance is observed near 1.4 eV, consistent with a free-carrier plasma resonance. Although the reflectance is qualitatively like that expected for a metal, the optical conductivity $\sigma(\omega)$ and the real dielectric function $\varepsilon_1(\omega)$ are not typical of normal Drude behavior; at long wavelengths, $\sigma(\omega)$ is suppressed below the extrapolated Drude function with a peak around 0.2 eV, and $\varepsilon_1(\omega)>0$ below 0.2 eV. These anomalous features arise from residual molecular scale disorder in PANI-CSA. A quantitative analysis is given in terms of conduction-band parameters derived from the localization-modified Drude model. The results are consistent with the results of band calculations.[7] However, since we find that the mean free path $\Lambda \simeq 7$ Å is comparable to the unit-cell distance along the conjugated chain, PANI-CSA is a disordered metal close to the metal-insulator boundary.

## II. EXPERIMENTAL PROCEDURE

### A. Sample preparation

PANI-CSA was prepared by mixing 1.092 g m (0.012 M) of emeraldine base with 1.394 g m (0.006 M) of camphor sulfonic acid (CSA) in agate mortar and pestle in a glove bag filled with nitrogen gas. The molar ratio of CSA to phenyl-nitrogen repeat unit was 0.5 for complete protonation of the polyaniline to the emeraldine salt form.[26–29] High-quality films of PANI-CSA were obtained by casting the material from solution in meta-cresol;[26–29] the solution was prepared by adding an appropriate quantity of PANI-CSA to meta-cresol (e.g., 1.0 g of PANI-CSA to 24 g of meta-cresol to yield a 3.9% solution). The mixture was treated in an ultrasonic bath for 48 h and subsequently centrifuged. Free-standing PANI-CSA films were obtained by casting onto glass plates and drying in air for 24 h on a hot plate at 50 °C. Lustrous dark free-standing films are then peeled from the glass plates. The surface quality of these films was sufficient for absolute measurements of the reflectivity without concern for scattering losses. Film thicknesses were typically 50–90 $\mu$m, sufficiently greater than the electromagnetic penetration depth to avoid the transmittance of the incident radiation. Since the PANI-CSA was cast from solution, the PANI chains are neither chain extended nor chain aligned. In this sense, the films can be considered isotropic, revealing no preferred direction.

The film preparation conditions for all PANI-CSA samples used in this experimental study were more or less identical. Nevertheless, subtle changes in morphology and crystallinity in the films (dependent on factors such as the concentration of the solution from which the films are cast, the rate of evaporation of the solvent, the thickness of the film, etc.) lead to corresponding changes in the electrical properties. Although the room-temperature conductivities of PANI-CSA films are not very much affected by such details of the film casting process, the low-temperature transport properties are quite sensitive to these factors.[28,29] Since scanning electron micrographs show no major differences in morphology in the various films, up to 0.1-$\mu$m resolution, the observed differences in the transport result from molecular scale to nanoscale changes in the disorder.

In this reflectance study, we have examined six different films with transport properties indicative of all three regimes: the critical regime, the metallic state near the critical regime, and the insulating state near the critical regime (see Refs. 28 and 29 for details). Except for the lowest photon energies, the IR reflectance data were insensitive to the subtle differences in transport behavior (e.g., below 0.2 eV, the optical conductivity extrapolates to the dc value; see Sec. IV). The general features of the reflectance spectrum were reproducible and observed in all samples.

### B. Optical measurements

Reflectance measurements were performed between 50 and 50 000 $cm^{-1}$ (0.006–6 eV) using two different spectrometers. Infrared reflectance spectra in the range of 50–9000 $cm^{-1}$ (0.006–1.1 eV) were measured with a Nicolet Magna-750 Fourier Transform Interferometer with a variety of light sources, beam splitters, and detectors for different overlapping frequency ranges. Visible/UV (VIS/UV) range spectra (0.5–6.0 eV) were obtained using a Perkin-Elmer Lambda-9 grating monochrometer. The overlap between spectral regions obtained with different instruments was excellent. The absolute value of reflectivity was determined by comparison with a Au (IR) or an Al (VIS/UV) reference mirror; the data were corrected using the absolute values of the reflectance of the reference as given in the literature.

The sample and the reference mirror were mounted on a helium-cooled cold finger, along with a thermometer and a resistance heater, to allow the temperature to be varied from 10 to 350 K. The sample and reference could be exchanged (for determination of the absolute reflectivity) by rotating the cryostat. The angle of incidence of the reflectance accessories is approximately 10°. Since the details of the reflectivity are very critical to the Kramers-Kronig analysis, we carefully tested the stability and the absolute reflectance at each temperature.

The agreement of the spectra from different instruments (within the overlap frequency range) was typically within 0.5%. The experimental uncertainty in our reflectance measurements is estimated to be ±0.5%, arising mainly from the difficulty in establishing precise optical alignment when the reference and sample are interchanged.

The optical conductivity and dielectric constants were obtained by Kramers-Kronig (KK) transformation of the reflectance spectra. In principle, the KK transformation requires a knowledge of reflectivity spectrum at all frequencies. Since data are available from the limited spectral range from 0.006 to 6 eV, reasonable and careful extrapolations of the reflectivity have been made beyond the measurement range: between 6 and 35 eV ($6 < \hbar\omega < 35$ eV), the data were continued by a $\omega^{-2}$ extrapolation, while the high-energy part above 35 eV was approximated with $\omega^{-4}$ (the asymptotic behavior of free electrons). This extrapolation had little effect on the low-frequency dependences of $\sigma(\omega)$ and $\varepsilon(\omega)$; the parameters of principal concern for establishing the details of the metal physics. At lower frequencies ($\hbar\omega < 0.006$ eV), the reflectivity was extrapolated toward zero frequency by means of the Hagen-Rubens relation.

## III. RESULTS AND ANALYSIS

### A. Reflectivity

Figure 1 shows the reflectivity spectra (0.006–6.0 eV) of a free-standing PANI-CSA film at 10 and 300 K. At 10 K, the reflectance is greater than 80% in the far IR ($\omega \leq 100$ cm$^{-1}$) and drops rapidly throughout the mid-IR to a minimum near 1.4 eV. This 1.4-eV minimum is indicative of a free-carrier plasma resonance characteristic of metal-like behavior. Above the minimum, the spectrum is featureless to 6 eV, except for the weak structure around 2.8 eV associated with the interband transition (well known in absorption spectra).[4,6,7,30]

The high reflectance in the far IR and the plasma resonance near 1.4 eV are traditional signatures of metallic behavior.[31] These characteristic spectral features show only weak temperature dependence; the reflectivity in the far IR is somewhat lower at 300 K than at 10 K. There are no significant spectral changes (at different temperatures) above 4000 cm$^{-1}$ (0.5 eV). Obvious phonon features appear throughout the IR (500–2000 cm$^{-1}$). Since the phonon features are completely screened in highly conducting metals[32] (due to the strong Drude-type response of the free carriers), the appearance of the phonon modes implies that PANI-CSA is marginally metallic, i.e., close to the disorder-induced metal-insulator transition. A detailed study and assignment of the IR phonon modes are in progress.

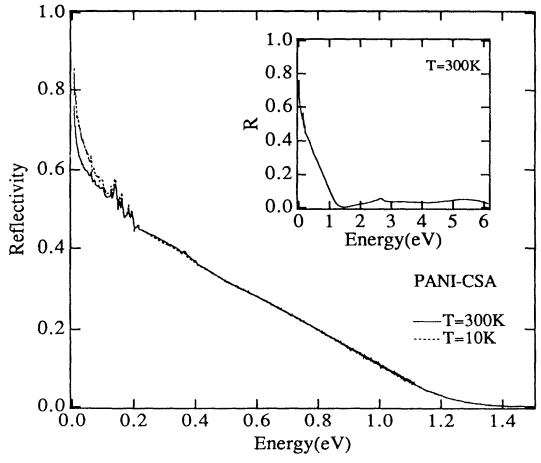


FIG. 1. Reflectivity spectra of PANI-CSA free-standing films measured at room temperature (solid curve) and 10 K (dotted curve). The inset shows the full spectrum as measured up to 6 eV.

### B. Optical conductivity

The implications of the reflectivity spectra become clear when the optical conductivity $\sigma(\omega) = \omega\varepsilon_2/4\pi$ is obtained through the Kramers-Kronig (KK) transformation. Figure 2 shows $\sigma(\omega)$ over the spectral range below the 1.5 eV. Although the results imply intraband Drude-like excitations centered at $\omega = 0$ (there is no energy gap), the optical conductivity deviates from the normal Drude behavior at low energies; below about 0.2 eV, $\sigma(\omega)$ decreases toward the dc value (with phonon features superposed). In fact, the conductivity extrapolated to $\omega = 0$ is in good agreement with that actually measured on this sample ($\sigma = 230$ S/cm). This low-frequency behavior arises from molecular scale disorder; PANI-CSA is near the border of the Anderson metal-insulator transition.

Above the 1.4-eV minimum, $\sigma(\omega)$ starts to increase again around 2.5 eV, corresponding to the onset of interband transition, and evolves a peak at 2.8 eV. The 2.8-eV

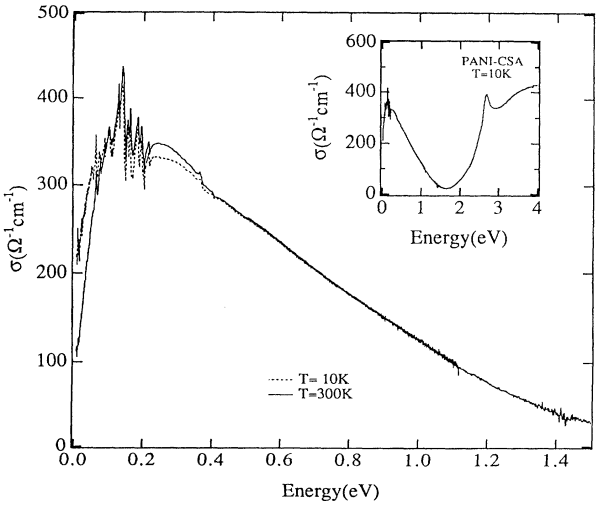


FIG. 2. Optical conductivity $\sigma(\omega)$ of PANI-CSA obtained from Kramers-Kronig transformation of the reflectivity data for 10 (dotted line) and 300 K (solid line). The inset shows $\sigma(\omega)$ over the extended spectral range up to 4 eV, including the low-frequency intraband (metal-like) contribution and the onset of the lowest interband transition near 2.5 eV.

peak is consistent with previous spectroscopic results obtained from the emeraldine salt.[4,6,7,30] For a metal, the onset of interband absorption is associated with transitions from the Fermi surface to the next-higher empty band, or with transitions from a lower-lying filled band to the Fermi surface.[31] Based on the band calculations,[7] the 2.8-eV peak corresponds to the transition from the second-highest valence band to the polaron band containing the Fermi surface. The pronounced peak previously observed at 1.5 eV, however, is not evident in the PANI-CSA spectrum.[4,6,30]

In the far IR, the optical conductivity at 10 K is somewhat higher than that at 300 K. The magnitude of the change is relatively small, consistent with the weak temperature dependence observed in direct current measurements.[28,29] Note that between 0.2 and 0.4 eV, $\sigma(\omega)$ shows the reverse behavior, so that the oscillator strength sum rule is satisfied. The data above 0.5 eV are independent of temperature.

### C. Dielectric functions and energy-loss function

The dielectric function $\varepsilon(\omega)=\varepsilon_1+i\varepsilon_2$ and the loss function $\mathrm{Im}[-1/\varepsilon(\omega)]$ can also be obtained by KK transformation of the reflectivity spectrum. The real and imaginary parts of the dielectric functions are shown (for energies below 2.0 eV) in Fig. 3. The real part of the dielectric function crosses zero at 0.8 eV. Below 0.8 eV, $\varepsilon_1$ is negative, as expected for a metal, where $\varepsilon_1(\omega)$ crosses zero at screened plasma frequency,[33] given by $\omega_p=\Omega_p/(\varepsilon_\infty)^{1/2}$, where $\Omega_p$ is the plasma frequency, $\Omega_p=[4\pi ne^2/m^*]^{1/2}$, $n$ is the number of electrons per unit volume with effective mass, $m^*$, and $\varepsilon_\infty$ is the high-frequency dielectric constant. However, in contrast to simple Drude behavior, the real part of dielectric function crosses zero again at still lower energies, and becomes positive for $\hbar\omega<0.2$ eV. This low-energy zero crossing in $\varepsilon_1(\omega)$ occurs near the maximum in $\sigma(\omega)$ (Fig. 2).

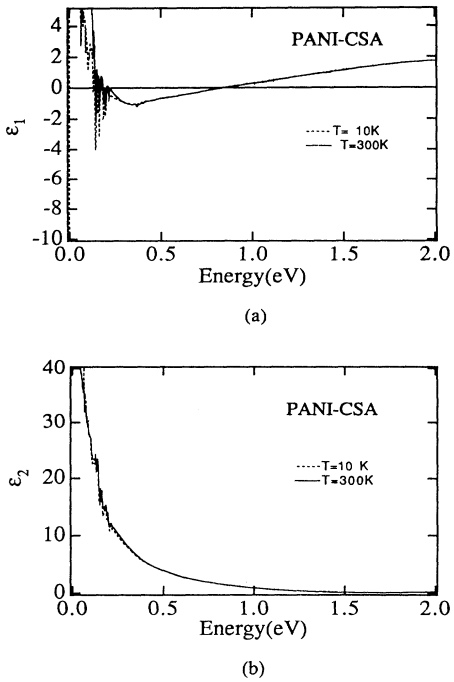


FIG. 3. (a) The real and (b) imaginary parts of the dielectric function, $\varepsilon(\omega)=\varepsilon_1+i\varepsilon_2$, of PANI-CSA obtained from Kramers-Kronig transformation of the reflectivity data. Note that the real part of the dielectric function crosses zero twice, at $\sim$0.8 eV and again at $\sim$0.2 eV; $\varepsilon_1(\omega)$ is a positive value below 0.2 eV.

The energy-loss function shown in Fig. 4 exhibits a well-defined peak with maximum at 1.1 eV. The maximum in $\mathrm{Im}[-1/\varepsilon(\omega)]$ and the reflectivity minimum are indicative of the existence of a damped plasma edge.[31] In simple metals, the maximum of the loss function occurs near $\Omega_p$; collective plasma oscillations occur at energies where $\mathrm{Im}[-1/\varepsilon(\omega)]$ is large and where $\varepsilon_1$ and $\varepsilon_2$ are both small.[34] The plasma resonance can be distinguished from an interband transition by the fact that both $\varepsilon_1$ and $\varepsilon_2$ are small in the vicinity of the maximum in the loss function.

### D. Effective number of carriers: $N_{\mathrm{eff}}(\omega)$

The integrated spectral weight $N_{\mathrm{eff}}(\omega)$ provides information on the free carriers responsible for the Drude-like contribution to $\sigma(\omega)$:

$$N_{\mathrm{eff}}(\omega)=\frac{2m^*V}{\pi e^2}\int_0^{\omega}\sigma(\omega')d\omega' , \tag{1}$$

where $N_{\mathrm{eff}}(\omega)$ is the effective number of carriers per unit cell contributing to the conductivity at frequencies below $\omega$, and $V$ is the unit-cell volume. In calculating $N_{\mathrm{eff}}(\omega)$, we have used the approximate unit-cell dimensions $a=5.9$ Å, $b=10$ Å, and $c=7.2$ Å, taken from the x-ray-diffraction analysis for the unit-cell volume of PANI-CSA.[35] The effective mass of electron ($m^*$) was assumed to be the free-electron mass $m_e$. Figure 5 illustrates the $N_{\mathrm{eff}}(\omega)$ calculated from $\sigma(\omega)$ for $T=10$ and 300 K;

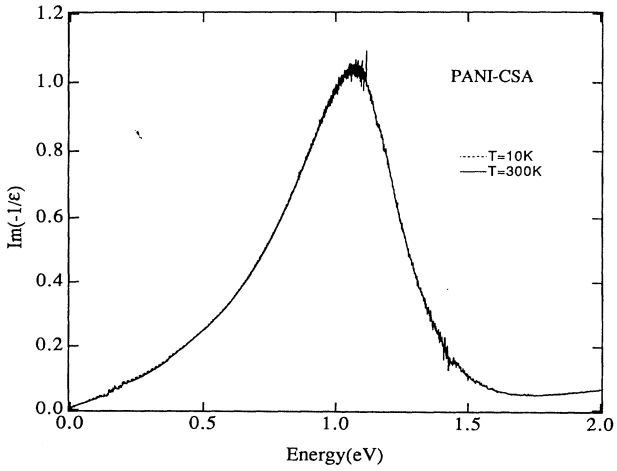


FIG. 4. Energy-loss function $\mathrm{Im}[-1/\varepsilon(\omega)]$ of PANI-CSA calculated from the real and imaginary parts of the dielectric function.

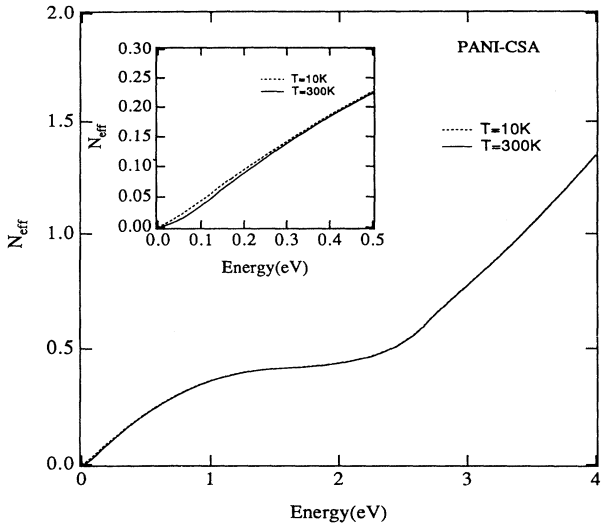


FIG. 5. The effective number of carriers per unit cell, $N_{\text{eff}}(\omega)$, as a function of energy. The effective mass was assumed to be equal to the free-electron mass. The inset shows the low-energy region with an expanded scale.

$N_{\text{eff}}(\omega)$ increases up to 1.2 eV followed by saturation above 1.2 eV. Thus the free-carrier oscillator strength is almost fully contained on $\sigma(\omega)$ below the plasma frequency, as in a simple metal. Above 1.2 eV, $N_{\text{eff}}$ remains constant up to $\approx 2.5$ eV, above which it increases again due to the onset of the interband transition.

From the saturation value above 1.2 eV, we obtain an estimate of the effective number of carriers per unit cell involved in the intraband Drude-like contribution to $\sigma(\omega)$; $N_{\text{eff}}(\omega) \cong 0.5$ per unit cell (two rings) when $m^*$ is taken as the free-electron mass $m_e$. Since the chemistry quite clearly indicates one free carrier per unit cell, we conclude that the optical mass (the effective mass averaged over the occupied states) is approximately $2m_e$. The resulting value for $N_{\text{eff}}$ yields a charge-carrier density of $2.4\times10^{21}$ cm$^{-3}$, in excellent agreement with the $2.3\times10^{21}$ cm$^{-3}$ obtained from theory based on the calculated band structure[7] and magnetic susceptibility.[8,9]

As illustrated again in the $N_{\text{eff}}(\omega)$ plots, only a minor difference is observed in the far IR between the curves obtained from the 10- and 300-K data. Furthermore, the two curves come together nicely at frequencies above 0.5 eV, demonstrating quantitatively the conservation of oscillator strength. Increasing the temperature does not affect the total spectral weight, but rather causes a slight redistribution of the spectral weight, as required by the oscillator strength sum rule.[34]

### E. Localization-modified Drude model

Although the overall spectral response of PANI-CSA at low energies can be attributed to free-carrier intraband excitations, $\sigma(\omega)$ and $\varepsilon_1(\omega)$ are not typical of normal Drude-like behavior below 0.2 eV. Detailed analysis of the direct current transport data has demonstrated that PANI-CSA is a disordered metal close to the metal-insulator boundary.[28,29] Thus we attribute the anomalous behavior of $\sigma(\omega)$ and $\varepsilon_1(\omega)$ below 0.2 eV to disorder-induced localization, and we analyze the results in terms of the localization-modified Drude model introduced by Mott.[22,23]

In simple metals where the mean free path is much greater than the lattice constant, the Drude model accurately describes the frequency-dependent conductivity

$$\sigma_{\text{Drude}}(\omega)=\frac{\Omega_p^2\tau}{4\pi(1+\omega^2\tau^2)} . \tag{2}$$

Mott and Kaveh[21] proposed that in the regime of weak disorder-induced localization, the Drude model should be modified; the first-order correction is given by the following:[21–23]

$$\sigma(\omega)=\sigma_{\text{Drude}}(\omega)\left[1-\frac{C}{(k_F\Lambda)^2}\left[1-\frac{\Lambda}{L_\omega}\right]\right] , \tag{3}$$

where $\Lambda$ is the mean free path ($\Lambda=v_F\tau$ and $v_F$ is the Fermi velocity), $k_F$ is the Fermi wave vector, and $L_\omega$ is the distance scale over which an electron diffuses within a period of the incident radiation field. The constant $C$ is not known exactly, but the magnitude of $C$ is of order unity. The value of $L_\omega$ is given by the diffusion coefficient, $D=\Lambda^2/3\tau$, and the optical frequency $\omega$ using the diffusion equation

$$L_\omega=(D/\omega)^{1/2} . \tag{4}$$

Equation (3) can be expressed alternatively as follows:

$$\sigma(\omega)=\frac{\Omega_p^2\tau}{4\pi(1+\omega^2\tau^2)}\left[1-\frac{C}{(k_Fv_F)^2\tau^2}+\frac{C}{(k_Fv_F)^2\tau^{3/2}}(3\omega)^{1/2}\right] . \tag{5}$$

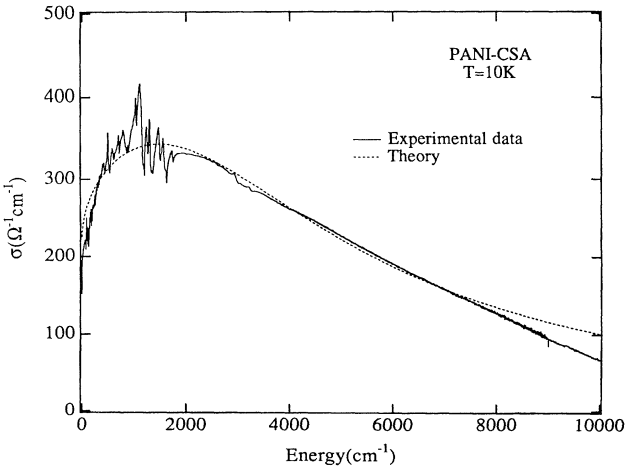


FIG. 6. The optical conductivity $\sigma(\omega)$ (solid line) of PANI-CSA is compared with that calculated (dashed line) from the localization-modified Drude model as described in Eq. (5), with the following parameters: $\Omega_p=9970$ cm$^{-1}$, $1/\tau=4340$ cm$^{-1}$, and $C/(k_Fv_F)^2=0.622\times10^{-30}$ s$^2$.

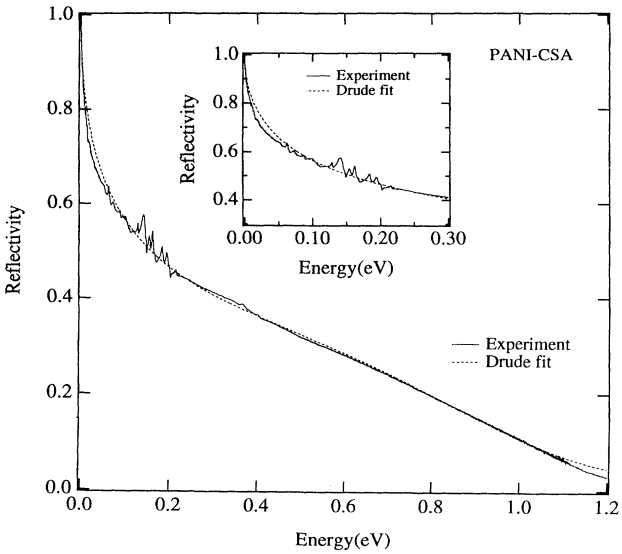


FIG. 7. The reflectivity spectrum (solid line) of PANI-CSA as shown in Fig. 1 is compared with that calculated by the Drude model using $\Omega_p=9970$ cm$^{-1}$, and $1/\tau=4340$ cm$^{-1}$ (the same parameters as used in Fig. 6).

Equation (5) is in good agreement with the measured optical conductivity in the intraband region below 1 eV, as shown in Fig. 6. The best fit is obtained with the following parameters: $\Omega_p=9970$ cm$^{-1}$ (1.17 eV), $1/\tau=4340$ cm$^{-1}$ (0.51 eV), and $C/(k_F v_F)^2=0.622\times10^{-30}$ s$^2$.

The parameters obtained from the localization-modified Drude fit are reasonable. The plasma frequency is close to that obtained from the reflectance minimum ($\approx1.4$ eV) and the peak in the loss function ($\approx1.1$ eV). For comparison, we show the simple Drude fit to the measured reflectivity in Fig. 7, using $\Omega_p=9970$ cm$^{-1}$, and $1/\tau=4340$ cm$^{-1}$. Deviations between the Drude fit and the data can be seen only at the lowest energies (below 0.2 eV), where the effect of weak localization is dominant.

## IV. DISCUSSION

### A. "Metallic" conductivity of PANI-CSA

The Drude parameters given above provide an estimate of the intrinsic conductivity at room temperature, i.e., the conductivity that would be obtained if the disorder did not limit $\sigma(\omega)$ for energies below 0.2 eV. Using $\sigma(0)=(1/4\pi)\Omega_p^2\tau$, with $\Omega_p=9970$ cm$^{-1}$ and $1/\tau=4340$ cm$^{-1}$, we obtain $\sigma(0)\approx400$ S/cm for the nonoriented sample. This value is a little higher than the measured dc conductivity in this sample at room temperature ($\sigma=230$ S/cm). However, if we evaluate the dc conductivity by the localization-modified Drude model, given as the $\omega=0$ limit of Eq. (5),

$$\sigma(0)=\sigma_{\text{Drude}}(0)\{1-C/[(k_F v_F)^2\tau^2]\}\ , \tag{6}$$

where $C/(k_F v_F)^2$ is estimated to be $0.622\times10^{-30}$ s$^2$ and $1/\tau=4340$ cm$^{-1}$, one finds $\sigma(0)\approx220$ S/cm, in excellent agreement with the measured dc conductivity.

### B. Fermi velocity and mean free path from the localization-modified Drude model

One can use the parameter $C/(k_F v_F)^2\approx0.622\times10^{-30}$ s$^2$ obtained from the fit to the localization-modified Drude model to estimate the mean free path at room temperature. Assuming that $C$ is of order of unit and that $k_F=\pi/2c$, where $c=7.2$ Å, one finds $v_F\approx5.6\times10^7$ cm/s. With $\tau=1.22\times10^{-15}$ s, one obtains $\Lambda\approx7$ Å, which is comparable to the unit-cell distance along the conjugated chain. This result clearly demonstrates that the PANI-CSA is near the metal-insulator transition, in agreement with the conclusions obtained from transport and magnetoresistance measurements.[28,32]

For a half-filled one-dimensional band, the density of states at the Fermi energy $N(E_F)$, can be expressed as follows:

$$N(E_F)=2/\pi\hbar v_F\ . \tag{7}$$

Note that although the relevant band is three-quarters filled, the existence of two phenyl rings per repeat unit leads to a degeneracy at the zone boundary.[7] Thus the density of states is properly expressed as that for a half-filled one-dimensional band. Using Eq. (7), one finds $N(E_F)\approx1.2$ state per eV per formula unit. Since $N(E_F)$ is closely related to the bandwidth $W$, $N(E_F)=4/\pi cW$, where $c$ is the lattice constant, the bandwidth can be estimated as approximately 1 eV, consistent with the band calculation result.[7] Furthermore, the Fermi energy $E_F$ is calculated to be 0.4 eV. These optically determined band parameters compare favorably with values derived from other low-energy experiments.[26–29,36] This good agreement confirms the validity of the localization-modified Drude model to PANI-CSA.

### C. Weak localization in PANI-CSA

The conclusion that the mean free path is comparable with the repeat unit along the $\pi$-conjugated chain supports the fact that PANI-CSA is on the metal-insulator boundary and approaching the Ioffe-Regel limit. Since the overall spectral response at low energies is dominated by the intraband excitations, there is no gap in the electronic density of states; PANI-CSA can be viewed in the context of "Fermi glass."

The deviations from simple Drude behavior in the far IR are quantitatively consistent with the localization-modified Drude model[22,23] and consistent with predictions for a weakly disordered system based upon the scaling theory of localization.[24] Similar behavior has been observed in disordered semiconductors close to the metal-insulator transition.[37]

As indicated by Eq. (5), localization depresses $\sigma(\omega)$ below the Drude curve in the far IR. Conservation of oscillator strength therefore, requires, that $\sigma(\omega)$ would be larger than the Drude curve at higher energies. The result that disorder can enhance the conductivity at intermediate frequencies was suggested by Mott, who argued that the spatial reduction of the electron wave function in some regions in the disordered metal must lead to a pile-up in other regions.[21–23] This pileup would imply an

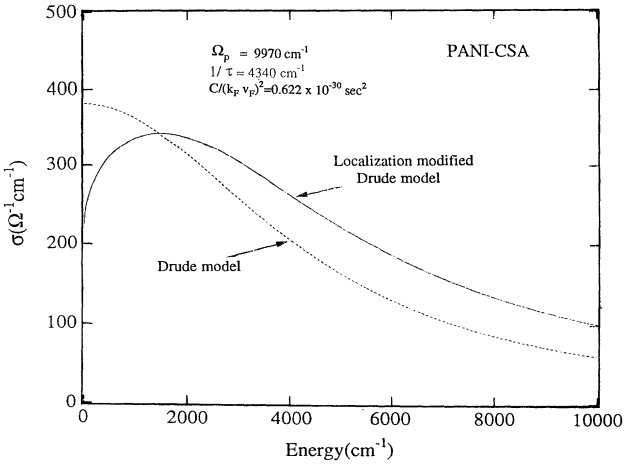


FIG. 8. The optical conductivity calculated from the localization-modified Drude model as described in Eq. (5) (solid line) and that calculated with the simple Drude model (dashed line) are compared. The same parameters were used in both cases: $\Omega_p = 9970\ \text{cm}^{-1}$, $1/\tau = 4340\ \text{cm}^{-1}$, and $C/(k_F v_F)^2 = 0.622 \times 10^{-30}\ \text{s}^2$.

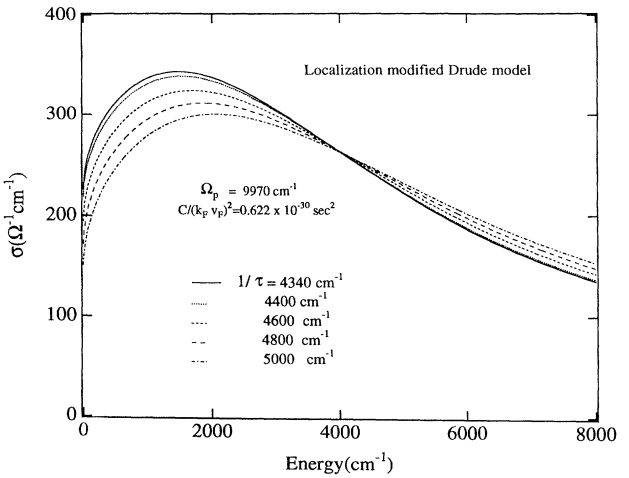


FIG. 9. The optical conductivities calculated from the localization-modified Drude model with different values for the scattering rate ($1/\tau$).

enhanced conductivity if the system is probed at the appropriate length scales.

The predicted enhancement of $\sigma(\omega)$ can be seen clearly in Fig. 8; the dashed line is the Drude prediction with the same fit parameters as the localization-modified model. At low frequencies, the localization-modified Drude model falls below the Drude curve, crossing over near the maximum in $\sigma(\omega)$ to values greater than the Drude curve throughout the mid-IR. Although this enhancement in conductivity has been observed in an alternating $n$-type/insulating GaAs heterostructure,[38] to our knowledge PANI-CSA is the first conducting polymer system to exhibit such behavior.

Using the mean free path estimated in Sec. III C, $\Lambda \approx 7$ Å, one finds $k_F \Lambda \approx 1.6$, indicating again that the PANI-CSA is not a good metal. The distance scale over which an electron diffuses within a period of the incident radiation field, $L_\omega = (D/\omega)^{1/2}$, is approximately 7 Å at 0.2 eV (using $D = \Lambda^2/3\tau$), comparable with the mean free path.

In the far IR, the optical conductivity is higher for the sample of 10 K than at 300 K. In the localization-modified Drude model, the only temperature-sensitive fitting parameter is the relaxation time $\tau$ [see Eq. (5)]. In an attempt to simulate the effect of increasing the temperature, in Fig. 9 we show a series of plots using Eq. (5) with different values for $1/\tau$. The qualitative features are in agreement with the data for PANI-CSA (see Fig. 2). The increase in $1/\tau$ with increasing temperature is consistent with a significant contribution from inelastic scattering due to phonon absorption. Note, however, that at frequencies greater than the Debye frequency, temperature-independent phonon emission will also contribute to $1/\tau$. Presumably this is the reason that $\sigma(\omega)$ is independent of temperature at energies above the characteristic phonon frequencies.

## V. CONCLUSION

In conclusion, the optical spectra of PANI-CSA are characterized by the metal-like behavior in the infrared due to intraband excitations: the Drude-like free-carrier excitations in the far-IR, and the existence of plasma resonance around 1.2 eV. Although the spectral response throughout the IR results from intraband excitations, the optical conductivity and the real part of the dielectric function are not typical of a Drude metal; the optical conductivity is suppressed at $\omega \rightarrow 0$ with a peak around 0.2 eV, and the real part of the dielectric function is positive below 0.2 eV. These features arise from the residual molecular scale disorder in PANI-CSA, resulting in weak localization. The localization-modified Drude model is in excellent agreement with the data; the analysis leads to the evaluation of the bandwidth, $W \approx 1$ eV, and the density of states at the Fermi energy, $N(E_F) \approx 1.2$ state per eV per formula unit, both of which are in good agreement with the electronic structure calculations.[7] The mean free path $\Lambda \approx 7$ Å is comparable to the unit-cell dimension along the conjugation axis, implying that PANI-CSA is a disordered metal near the metal-insulator boundary.

## ACKNOWLEDGMENTS

We thank Dr. Reghu Menon, Dr. C. O. Yoon, Dr. N. S. Sariciftci, and C. H. Lee for helpful discussions and for advice on details of the analysis. This work was supported by the MRL program of the National Science Foundation under Award No. DMR-9123048.

[1]A. J. Heeger, S. A. Kivelson, J. R. Schrieffer, and W. P. Su, Rev. Mod. Phys. **60**, 781 (1988).

[2]*Handbook of Conducting Polymers,* edited by T. A. Skotheim (Marcel Dekker, New York, 1986), Vol. 2, and references therein.

[3]W. R. Salaneck, I. Lundstrom, W.-S. Huang, and A. G. MacDiarmid, Synth. Met. **13**, 291 (1986).

[4]Y. Cao, P. Smith, and A. J. Heeger, in *Conjugated Polymeric Materials: Opportunities in Electronics, Optoelectrics and Molecular Electronics,* Vol. 82 of *NATO Advanced Study Institute, Series E: Applied Sciences,* edited by J. L. Bredas and R. R. Chance (Kluwer Academic, Dordrecht, 1990).

[5]A. G. MacDiarmid and A. J. Epstein, in *Science and Applications of Conducting Polymers,* edited by W. R. Salaneck, D. T. Clark, and E. J. Samuelson (Hilger, Bristol, 1991), p. 117.

[6]F. Wudl, R. O. Angus, F. L. Lu, D. M. Allemand, D. J. Vachon, M. Nowak, Z. X. Liu, and A. J. Heeger, J. Am. Chem. Soc. **109**, 3677 (1987).

[7]S. Stafstrom, J. L. Bredas, A. J. Epstein, H. S. Woo, D. B. Tanner, W. S. Huang, and A. G. MacDiarmid, Phys. Rev. Lett. **59**, 1464 (1987); D. S. Boudreaux, R. R. Chance, J. F. Wolf, L. W. Shacklette, J. L. Bredas, B. Themans, J. M. Andre, and R. S. Silbey, J. Chem. Phys. **85**, 4584 (1986).

[8]C. Fite, Y. Cao, and A. J. Heeger, Solid State Commun. **73**, 607 (1990).

[9]Y. Cao and A. J. Heeger, Synth. Met. **52**, 193 (1992).

[10]Y. Cao (unpublished).

[11]A. J. Epstein, J. M. Ginder, F. Zuo, H.-S. Woo, D. B. Tanner, A. F. Richter, M. Angelopoulos, H.-S. Huang, and A. G. MacDiarmid, Synth. Met. **21**, 63 (1987).

[12]J. M. Ginder, A. F. Richter, A. G. MacDiarmid, and A. J. Epstein, Solid State Commun. **63**, 97 (1987).

[13]Z. H. Wang, E. M. Scherr, A. C. MacDiarmid, and A. J. Epstein, Phys. Rev. B **45**, 4190 (1992); Z. H. Wang, C. Li, E. M. Scherr, A. G. MacDiarmid, and A. J. Epstein, Phys. Rev. Lett. **66**, 1745 (1991).

[14]Z. H. Wang, A. J. Epstein, A. Ray, and A. G. MacDiarmid, Synth. Met. **41-43**, 749 (1991).

[15]D. S. Galvao, D. A. dos Santos, B. Laks, C. P. de Melo, and M. J. Caldas, Phys. Rev. Lett. **63**, 786 (1989).

[16]Z. H. Wang, C. Li, E. M. Scherr, A. G. MacDiarmid, and A. J. Epstein, Phys. Rev. Lett. **66**, 1745 (1991).

[17]Qiming Li, Luis Cruz, and Philip Phillips, Phys. Rev. B **47**, 1840 (1993).

[18]H.-L. Wu and Philip Phillips, Phys. Rev. Lett. **66**, 1366 (1991).

[19]P. Sheng, B. Abeles, and Y. Arie, Phys. Rev. Lett. **31**, 44 (1973).

[20]A. L. Efros and B. I. Shklovskii, J. Phys. C **8**, L49 (1975).

[21]N. F. Mott and M. Kaveh, Adv. Phys. **34**, 329 (1985).

[22]N. F. Mott, in *Localization and Interaction in Disordered Metals and Doped Semiconductors,* edited by D. M. Finlayson, Proceedings of the Thirty-First Scottish Universities Summer School in Physics of 1986.

[23]N. F. Mott, in *Localization 1990,* edited by K. A. Benedict and J. T. Chalker, IOP Conf. Proc. No. 108 (Institute of Physics, and Physical Society, Bristol, 1990).

[24]P. A. Lee and T. V. Ramakrishnan, Rev. Mod. Phys. **57**, 287 (1985).

[25]N. F. Mott and E. Davis, *Electronic Processes in Non-Crystalline Materials* (Clarendon, Oxford, 1979).

[26]Y. Cao, P. Smith, and A. J. Heeger, Synth. Met. **48**, 91 (1992).

[27]Y. Cao, G. M. Treacy, P. Smith, and A. J. Heeger, Appl. Phys. Lett. **60**, 1 (1992).

[28]M. Reghu, Y. Cao, D. Moses, and A. J. Heeger, Phys. Rev. B **47**, 1758 (1993).

[29]M. Reghu, C. O. Yoon, Y. Cao, D. Moses, and A. J. Heeger, Phys. Rev. B (to be published).

[30]Y. Cao, P. Smith, and A. J. Heeger, Synth. Met. **32**, 263 (1989).

[31]H. Ehrenreich and H. R. Phillipp, Phys. Rev. **128**, 1622 (1962).

[32]For example, see T. Timusk and D. B. Tanner, in *Physical Properties of High Temperature Superconductors I,* edited by D. M. Ginsberg (World Scientific, Singapore, 1989), p. 339.

[33]C. Kittel, *Introduction to Solid State Physics* (Wiley, New York, 1976).

[34]See, e.g., F. Wooten, *Optical Properties of Solids* (Academic, New York, 1972).

[35]C. S. Yang, Y. Cao, P. Smith, and A. J. Heeger, Synth. Met. **53**, 293 (1993).

[36]C. O. Yoon, M. Reghu, Y. Cao, D. Moses, and A. J. Heeger, Phys. Rev. B **48**, 14 080 (1993).

[37]P. Dai, Y. Zhang, and M. P. Sarachik, Phys. Rev. B **45**, 3984 (1992); **46**, 6724 (1992); T. F. Rosenbaum, R. Milligan, G. A. Thomas, P. A. Lee, T. V. Ramakrishnan, and R. N. Bhatt, Phys. Rev. Lett. **47**, 1758 (1981).

[38]H. K. Ng, M. Capizzi, G. A. Thomas, R. N. Bhatt, and A. C. Gossard, Phys. Rev. B **33**, 7329 (1986).